Dynamics of Arthropod Filiform Hairs. II. Mechanical Properties of Spider Trichobothria (Cupiennius salei Keys.)

Friedrich G. Barth, Ute Wastl, Joseph A. C. Humphrey and Raghuram Devarakonda

Email alerting service	Receive free email alerts when new articles cite this article - sign up in the box at the top right-hand corner of the article or click **here**

Dynamics of arthropod filiform hairs.
II. Mechanical properties of spider trichobothria (*Cupiennius salei* Keys.)

FRIEDRICH G. BARTH[1], UTE WASTL[1], JOSEPH A. C. HUMPHREY[2] AND RAGHURAM DEVARAKONDA[2]

[1]*Institut für Zoologie, Universität Wien, Althanstr. 14, A-1090 Wien, Austria*
[2]*Department of Mechanical Engineering, University of California at Berkeley, Berkeley, California 94720, U.S.A.*

CONTENTS

SUMMARY

Adults of the wandering spider *Cupiennius salei* (Ctenidae) have 936 ($\pm$ 31 s.d.) trichobothria or filiform hairs on their legs and pedipalps. This is the largest number of these air movement detectors recorded for a spider. The trichobothria are 100–1400 μm long and 5–15 μm wide (diameter at base). Many of them are bent distally pointing towards the spider body. Their feathery surface increases drag forces and thus mechanical sensitivity by enlarging the effective hair diameter. Typically, trichobothria are arranged in clusters of 2–30 hairs which increase in length towards the leg tip.

The trichobothria's mechanical directionality is either isotropic or it exhibits a preference for air flow parallel or perpendicular (from lateral) to the long leg axis. These differences are neither due to the distal bend of the hair nor to the bilateral symmetry of the cuticular cup at the hair base but to the spring supporting the hair. Different directional properties may be combined in the same cluster of hairs.

Trichobothria are tuned to best frequency ranges between 40 and 600 Hz depending on hair length. Because, with increasing hair length, absolute mechanical sensitivity changes as well, the arrangement of hairs in a cluster provides for a fractionation of both the intensity and frequency range of a stimulus, in addition, in some cases, to that of stimulus direction.

Boundary layer thickness above the spider leg in oscillating airflow varies between about 2600 μm at 10 Hz and 600 μm at 950 Hz. It is well within the range of hair lengths. In airflow perpendicular to the long leg axis particle velocity above the leg increases considerably as compared to the free field. The curved surface of the cuticular substrate has therefore to be taken into account when calculating hair motion.

The experimentally measured properties of hair and air motion were also determined numerically using the theory developed in the companion paper (Humphrey *et al. Phil. Trans. R. Soc. Lond.* B **340**, 423–444 (1993)). There is good agreement between the two. Short hairs are as good or better velocity sensors as long hairs but more sensitive acceleration sensors. In agreement with most of our measurements optimal hair length is not larger than boundary layer thickness at a hair's best frequency. Best frequencies of hair deflection and of ratio *a* (maximum hair tip displacement:air particle displacement) differ from each other. The highest measured value for ratio *a* was 1.6. In only 22% of the cases hair tip displacement exceeded air particle displacement. Hair motion is insensitive to changes in hair mass as shown by the numerical comparison of a solid and a hollow hair.

445

1. INTRODUCTION

Air movement detectors in arthropods are best represented by insect filiform hairs such as those on the orthopteran cerci and by their arachnid equivalent, the trichobothria. In both these cases the hair shaft appears to be a light-weight structure whose articulation to the exoskeletal cuticle is extremely flexible. As a consequence the drag forces of moving air efficiently deflect the hair shaft at flow velocities as low as 1 mm s^{-1}, possibly less, and at frequencies as high as several hundred Hz.

Recent years have seen major progress in the interpretation of the physics underlying the mechanical operation of such movement detectors in insects (Fletcher 1978; Tautz 1978, 1979; Shimozawa & Kanou 1984a,b; Kämper & Kleindienst 1990). The companion paper to this (Humphrey et al. 1993) extends the available fluid mechanical theory of arthropod hairs and clarifies some important issues so far either neglected, in error or simply unresolved.

The present account deals with the mechanics of spider trichobothria which are not homologous to insect filiform hairs but of different phylogenetic origin. Trichobothria also differ from insect filiform hairs in the number of sensory cells innervating a hair, in the manner of their coupling to the sensory dendrites and their behavioural relevance as far as it is known (for a review, see Reißland & Görner (1985)). Trichobothria mechanics has so far been the subject of only two studies (Görner & Andrews 1969; Reißland & Görner 1978). These authors exposed the trichobothria of agelenid web spiders to stationary airflow and to both the farfield and nearfield of sound.

In addition to being different from insect filiform hairs, trichobothria vary considerably among different families and ecological types of spiders with regard to distribution, length and, presumably, sensitivity. Our own study uses the trichobothria of a large wandering spider dwelling on plants (Barth et al. 1988) instead of in a web. We strive to: (i) provide the basis for a more extensive analysis of the functional properties and behavioural role of this trichobothrial sensory system; and (ii) compare actual measurements with the predictions derived from the numerical model presented in the companion paper (Humphrey et al. 1993).

In the present paper we first describe details of number, arrangement, and shape of the trichobothria of *Cupiennius salei* (Ctenidae). We then ask for the mechanical directionality of the hairs and their motion in oscillating airflow. Our experimentally determined data turn out to fit very well the predictions made by our theoretical study (Humphrey et al. 1993).

2. MATERIAL AND METHODS

Animals

We used adults of the tropical wandering spider *Cupiennius salei* Keys. (Ctenidae; Barth et al. 1988; Lachmuth et al. 1984) throughout this study. The animals were bred and raised in the laboratory and were the offspring of spiders originally collected in Mexico.

Topography

Distribution and external morphology of the trichobothria were studied in five adult males and five adult females. Animals were anaesthetized using CO_2 and cooled to $-20°C$. Extremities carrying trichobothria were drawn using a camera lucida. Individual groups of trichobothria were also photographed. Methods applied for scanning electron microscopy (JEOL JSM T 300) were conventional.

Hair deflection in an oscillating sound field

Mechanical tuning and directional properties of individual hairs of four selected groups of trichobothria were examined in a controlled oscillating flow field. For this purpose identical loudspeakers (WS 17, Visaphon, diameter 14 cm) were mounted at both open ends of a horizontally oriented plastic cylinder (length 20 cm, diameter 15 cm) and driven in push-pull mode using a function generator (TOE 7708, Toellner) together with a digital frequency counter (SC 7201, Iwatsu). The resulting flow field was examined for homogeneity and calibrated with a laser Doppler anemometer kindly made available by J. Tautz, University of Konstanz, F.R.G. Air particle velocity turned out to be perfectly controllable with wall effects in the cylinder only relevant at distances smaller than 1 cm from the wall.

The leg to be examined was introduced into the centre of the cylinder with a micromanipulator. It was carefully oriented horizontally and parallel to the direction of air particle oscillation, and could be rotated in this plane for the measurement of hair directional properties. By definition, an orientation of 0° and 180° is parallel to the flow field. Individual trichobothria were observed and photographed under dark field illumination with a stereomicroscope (Wild M8) through a window cut into the plastic cylinder.

Legs to be examined were freshly autotomized and their open end carefully plugged with a mixture of bee's wax and colophony to slow down desiccation.

Hair deflection angles

Hair deflection angles α (1/2 of full deflection to both sides of zero position) were calculated from hair tip displacement x and hair length l (tan $α = x/l$). In the case of curved hairs l was taken as the distance between the cuticular surface and the point of the hair farthest away from that surface. Displacement of the hair tip could be determined with a precision of $±5$ μm or better. Taking a trichobothrium 1000 μm long the error in α amounts to up to $±0.14°$; taking a length of 500 μm it reaches $±0.29°$. The error in α resulting from the fact that the hair tip moves along an arc instead of along a straight horizontal line is negligible ($<1\%$) for the displacement angles relevant to this study ($\leqslant 10°$).

When measuring the tuning of individual trichobothria the longitudinal leg axis was always oriented parallel to the air flow. The frequencies chosen to generate particle velocities of 10, 20, 30, 40, and 50

Table 1. *Total number of experiments performed on the tuning and on the directionality of the trichobothria of Cupiennius salei*

(n_G, number of a particular group of trichobothria; n_T, number of individual trichobothria studied in the same group. See figure 1a for the definition of the four groups of trichobothria studied.)

	tuning		directionality intact hairs		shortened hairs	
	n_G	n_T	n_G	n_T	n_G	n_T
Tibia DAI	9	51	14	56	2	4
Tibia LP	9	43	11	40	2	4
Me Ta DI	9	42	18	73	3	5
TarsusD	3	11	5	14	4	7

mm s^{-1} were those for which we had calibrated the flow field (10, 40, 50, 100, 150, 250, 550, and 950 Hz). In addition, the velocities necessary to induce a given deflection angle (in most cases 2.5°) were determined. When measuring hair directionality with the leg oriented parallel to the flow field (0°) first the particle velocities necessary to deflect the hair by 1.25° or 5° were determined. Then the leg was rotated horizontally, particle velocity kept constant, and α measured at the different orientations of the leg (trichobothrium). A strobelight (1538-A Strobotac, General Radio) was used to find the frequency of a trichobothrium in the oscillating sound field.

All values in both tuning and directionality curves are means of five measurements obtained with the same trichobothrium of the same leg ($n = 5$, $N = 1$). Table 1 gives the total number of experiments, n_G representing the number of a particular group of trichobothria, and n_T the number of the individual trichobothria studied in the same group.

Boundary layers

Profiles of the maximum longitudinal velocity component (average) above the spider leg in oscillating air flow were measured with a laser Doppler anemometer (LDA, Dantec) in forward light scattering mode in the laboratory of J. Tautz, University of Konstanz, F.R.G. We used a 5 mW He-Ne-laser and room temperature smoke particles from incense sticks to get sufficient light scattering. As the leg was mounted on a micromanipulator, it could be moved in precise steps towards or away from the measuring volume of the LDA. The control volume of the intersecting laser beams had to be oriented at a right angle to the movement vector of the air particles in order to measure particle velocity parallel to the acoustical axis of the stimulating system. Zero position of the laser was defined as that position at which the measuring volume just touched the cuticular surface. Starting from this position the leg was moved away from the measuring volume in steps of 50 μm or 100 μm. A boundary layer thickness, defined according to

Prandtl & Tietjens (1934) as the distance from a surface at which 99% of the velocity in the free field (v_∞) is reached, was determined from each velocity profile.

Regarding our boundary layer measurements the reader is cautioned to note two inevitable methodological drawbacks: (i) The measuring volume could not be made smaller than $6 \times 0.6 \times 0.6$ mm^3 (rotation ellipsoid). Consequently, the measuring point closest to the cuticular surface is 0.3 mm above it. In addition, the velocity value obtained for a certain position results from the time integration of a sequence of velocity values associated with particles scattering light anywhere from within the entire measuring volume. (ii) The quality of the LDA signal suffers considerably from the presence of hairs and spines in the measuring volume, which therefore had to be removed. Although details of the velocity profile very close to the surface could not be determined we are confident about the boundary layer thickness measurements.

3. RESULTS

In this section we first present our experimental measurements and then proceed to analyse these with regard to the predictions based on the numerical model described in the companion paper (Humphrey *et al.* 1993).

(a) *Experimental*

(i) *Number and arrangement of trichobothria*

Adults of *Cupiennius salei* possess 936 ± 31 (mean ± s.d., $N = 10$) trichobothria. 100 ± 3 of these are found on each of the first and second, and 108 ± 3 on each of the third and fourth walking legs. The only consistent difference among the legs of the same individual is a group of trichobothria on the tibia (DA2, figure 1) only found on legs three and four. On each of the pedipalps there are only 52 ± 3 trichobothria (figure 1). These numbers are identical in males and females.

In walking legs the segments carrying trichobothria are the tarsus, metatarsus, and tibia. The pedipalpal trichobothria are all on the tibia. The large majority of trichobothria is found dorsally on the legs. The exceptions are two groups (five to eight trichobothria each) on the anterior and posterior aspect of the proximal tibia, respectively. The situation is similar in pedipalps. Also, the tibia of both walking legs and pedipalps shows the formation of groups of sensilla particularly well. These groups consist of between seven and 14 sensilla on the legs and of between three and 24 on the pedipalps (figures 1 and 2). All groups are identified and their positions on the respective segment are indicated by the abbreviations explained in figure 1.

Trichobothria on the metatarsus are more evenly distributed. They form a straight line of 23 to 37 sensilla dorsally along the midline of the leg segment. On the tarsus the trichobothria form a large dorsal group of up to 30 sensilla in an arrow shaped arrangement. This is the largest of all the groups in *Cupiennius*.
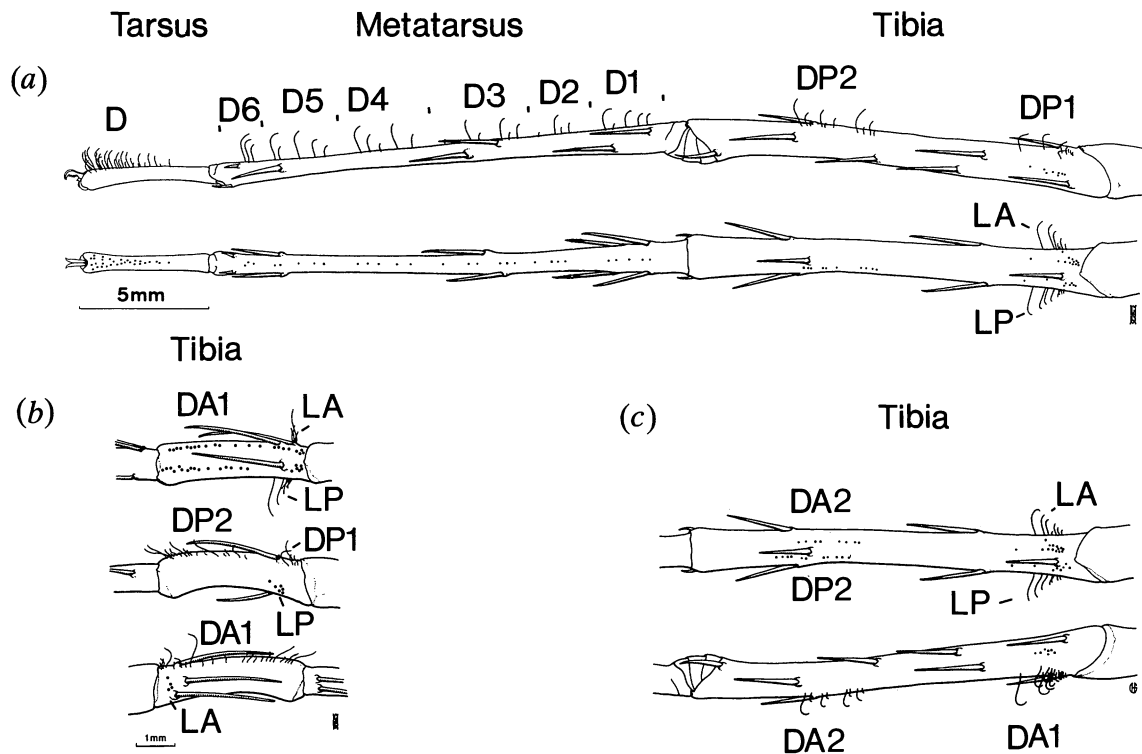
Figure 1. Arrangement of trichobothria of adult *Cupiennius salei*. (*a*) Dorsal and lateral view of left second walking leg. (*b*) Dorsal, posterior lateral, and anterior lateral view (from above to below) of left pedipalp. (*c*) Dorsal and lateral view of the tibia of left fourth walking leg. Abbreviations used to describe location of groups: D, dorsal; A, anterior; P, posterior; L, lateral.

(ii) *Hair structure*

Length

The most obvious variable among individual trichobothria is their length (figures 1 and 2). Within groups hair length increases from proximal to distal on the leg segment. In *C.salei* length varies between 100 μm and 1400 μm (1:14), typical values for the more extensively studied groups being 100–1200 μm (1:12, TiDA1), 150–1300 μm (1:9, TiLP), 175–850 μm (1:5, MeD1), and 125–1125 μm (1:9, TaD).

Curvature

The curvature of many trichobothria of *C. salei* (figures 1 and 2) is not an artifact due to desiccation in isolated legs but also observed in intact animals. It is usually the distal one third of the shaft which is bent towards the proximal end of the leg. The amount of bending tends to increase with hair length. Long trichobothria with particularly well pronounced curvature are those of group DA1 on the tibia.

The plane formed by a curved trichobothrium deviates from a plane parallel to the leg axis by 5° to 30°. Even more surprisingly, this deviation is not bilaterally symmetric with regard to the spider's long body axis but rotates with the leg axes around the spider. As a consequence the tips of the trichobothria point towards the posterior aspect of the leg on all right legs, and towards the anterior aspect on all left legs.

The cup

Trichobothrial hair shafts are surrounded by a cup-like cuticular structure at their bases. The opening of this cup (bothrium) is displaced distally (figure 3*a*). It is elliptical in cross section as is the overall shape of the bothrium when viewed from above. The mean ratio of the long diameter of the opening parallel to the leg axis to the shorter diameter perpendicular to it measures 1.3 ± 0.14 s.d. ($n = 107$) in the sensilla composing groups LP and DA1 on the tibia and group D1 on the metatarsus. Both the bilateral symmetry of the cup and its orientation along the long axis of leg and pedipalp are the same throughout and independent of the hair's preferred direction of movement (see below). However, both the overall length of the cup and its opening increase with hair length (figure 3*b*). Maximum hair deflection is limited by the outer rim of the cup. It measures 25° to 35° independent of hair length and cup size since the cup is deeper in a long hair than in a short hair (figure 3*c*). The inside of the sidewalls of the cup is grooved. The bottom of the cup is formed by the membrane suspending the hair shaft.

Hair shaft

The hair shaft of a trichobothrium is oriented roughly perpendicular to the leg or pedipalp surface (figure 2). Its most obvious morphological specialization is its feathery surface (figure 4). Whereas the cuticular protuberances are short (*ca.* 1 μm) close to the bothrium, they increase in length distally (up to *ca.* 6 μm). The density of their distribution decreases towards the hair tip.

In general, long hairs are thicker than short hairs. In all cases the diameter gradually decreases towards
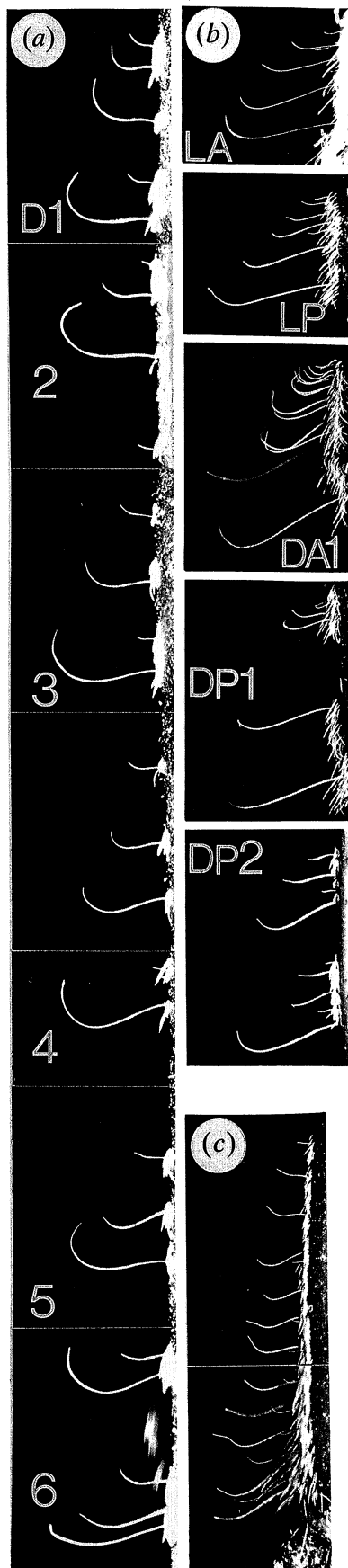
Figure 2. Trichobothria on walking leg. For abbreviations see figure 1; (*a*) metatarsus, (*b*) tibia, (*c*) tarsus. Magnification × 16.

the hair tip. Typically, long hairs measure 10–15 μm in diameter (including protuberances) at their base, whereas the equivalent value for short hairs is 5–7 μm. Tip diameters are up to 5 μm and only 1–2 μm, in long and short hairs, respectively.

(iii) *Mechanical directionality*

The directional properties of hair deflection were studied in the oscillating flow field in tibial groups DA1 and LP, metatarsal group D1, and tarsal group D. The hairs differ significantly from one another, depending on their position on the leg (figures 5 and 6).

The long trichobothria of TiDA1 and TiLP exhibit an almost isotropic deflectability. They show only a slight preference for directions perpendicular to the long leg axis, whereas this preference is very clear in the short hairs of the same groups (figure 5). In contrast, both long and short trichobothria of MeD1 are most easily deflected along the long axis of the leg (figure 6). Finally, the hairs of TaD again differ from each other. In this case the long distal hairs are maximally deflected by air movement perpendicular to the long leg axis whereas the preferred direction of the short proximal hairs is parallel to the long leg axis, similar to the metatarsal hairs (figure 6).

The shape of the directional response curve is independent of air movement frequency (10, 50, 150 Hz). It also remains unchanged in the case of curved trichobothria after cutting the curved part. Quite unexpectedly, in cut hairs only the overall absolute mechanical sensitivity (deflection) decreases (figure 7).

(iv) *Tuning*

These experiments were again done in the calibrated oscillating flow field. The deflection of both long and short hairs follows the stimulating frequency in a 1 to 1 fashion between 10 Hz and 950 Hz, which represents the whole range tested (correlation coefficient $r = 1$, $n = 8$).

The deflection angle, however, varies with stimulus frequency and it does so in different ways depending on hair length. This follows from experiments in which a certain maximal air particle velocity was kept constant and the frequency changed, and from experiments in which a certain deflection angle of the hair shaft was kept constant and the particle velocity necessary to elicit it was measured at different frequencies. With increasing hair length the range of best frequencies gradually shifts towards lower frequencies. Also, the slope of the curve below the range of best frequencies increases considerably with hair length. This will be discussed later with regard to the significance of velocity and acceleration, respectively, for hair motion (figures 8 and 9). Typically, these frequency curves are quite broad. Rather than giving a single best frequency it appears more appropriate to provide the 3 dB range to describe the underlying mechanical tuning. In all four groups of trichobothria tested these 3 dB ranges are much larger in short hairs than in long hairs. The 3 dB ranges of different hairs

(a)

(b)

$n = 107$

$y = 22 + 0.01 \cdot x$

$r = 0.8 \; p < 0.005$

cup length / μm

hair length / μm

$n = 107$

$y = 9.4 + 0.005 \cdot x$

$r = 0.8 \; p < 0.005$

cup opening / μm

hair length / μm

(c)

4 μm

α

7 − 9 μm

7 μm
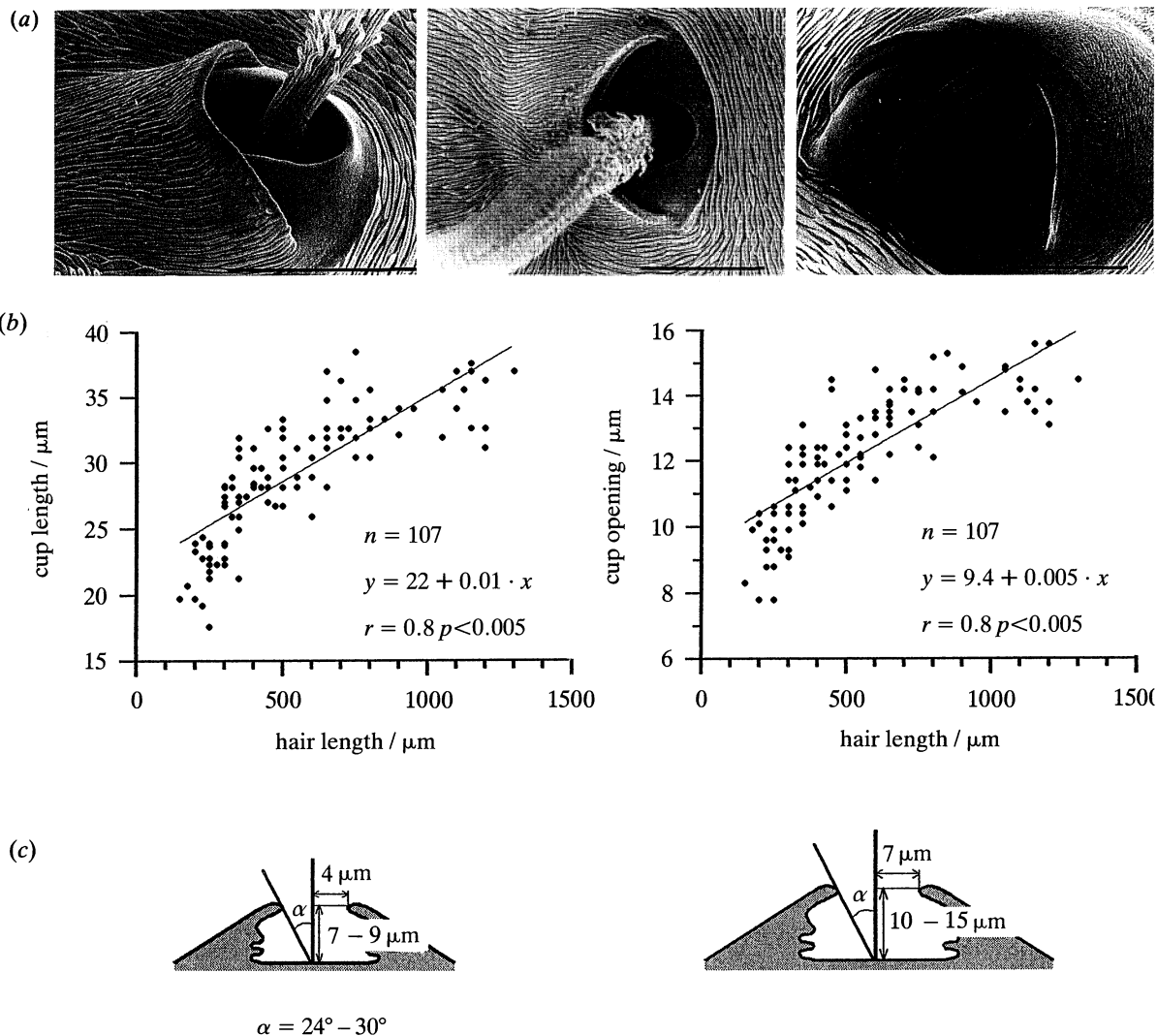
α

10 − 15 μm

$\alpha = 24° − 30°$

Figure 3. Structure of trichobothrial cup. (a) SEM views of cup of trichobothria of group TiLP (left, middle) and showing cuticular lamellae inside (right); scale 10 μm. (b) Relation between cup length and hair length. (c) Schematic longitudinal section through cup of a short (left) and of a long (right) hair. α, maximal angle of hair shaft displacement.

overlap considerably. Although it is difficult to associate a particular hair length with a particular best frequency, the centre frequencies of the 3 dB ranges as well as the individual single best frequencies clearly correlate with hair length within a particular group ($p < 0.005$; figure 10). As seen from figure 10 the frequency ranges for a given hair length are not identical in different groups; they are shifted towards higher frequencies in tibial groups DA1 and LP compared with both the metatarsal group D1 and tarsal group D. There is no obvious fluid mechanical explanation for this difference which we therefore propose to be due to a larger spring constant S and a smaller damping constant R in case of the tibial hairs (Humphrey *et al.* 1993, figure 12a).

When changing not only the frequency but also the maximum particle velocity, deflection angles (figure 11) again show a broad tuning. In addition, they demonstrate a linear relationship between deflection angle and particle velocity at different oscillation frequencies (figure 12).

(v) *Deflection and hair length*

At the same particle velocity (50 mm s^{-}) long hairs are deflected more than short ones at their respective best frequencies (figure 13). Thus, a hair of 1000 μm length of tibial groups DA1 and LP is deflected by 5°, whereas hairs of the same groups measuring only 500 μm are deflected by only 2.5°. The values found are significantly correlated to the linear regression curves shown in the graphs ($p < 0.05$).

Deflection of metatarsal (D1) and tarsal hairs (D) is significantly larger than that of tibial hairs (DA1, LP). The hairs of the more distally located groups are thus mechanically more sensitive than the more proximally located ones.

The ratios (a) of maximal hairtip deflection (x) at the best frequency to the maximal displacement of the oscillating air ($\xi = v/2 \cdot \pi \cdot f_i$; v, particle velocity at 50 mm s^{-1}; f, best frequency of trichobothrium; $a = x/\xi$) differ considerably among the trichobothria of all four groups examined. In tibial group DA1, metatarsal group D1, and tarsal group D, a is not correlated with
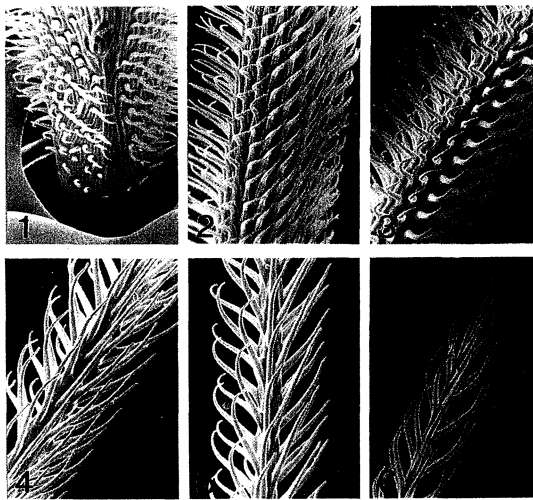
Figure 4. Surface structure of hairshaft. Photographs taken at different levels starting in cup (1) and ending at tip (6) of hair. Magnification × 1900.

(vi) *Velocity profiles*

Profiles of the average particle velocity above the leg in the oscillating flow field were measured by means of laser Doppler anemometry with the leg oriented parallel and perpendicular to the air movement vector, respectively. Boundary layer thickness was defined as the distance from the leg surface at which particle velocity assumes 99% of the value found in the free flow field (v_∞) (Prandtl & Tietjens 1934).

Leg parallel to flow field

The boundary layer thickness above the metatarsus at the site of group D1 clearly decreases with increasing frequency of the flow field (figure 15). Thus, it was as large as 2600 µm at 10 Hz and measured 1200 µm at 50 Hz and only 800 µm at 550 Hz. The differences in boundary layer thicknesses are particularly obvious between 10 Hz and about 150 Hz. Figure 15 presents the regression curve derived from all 26 measurements at the various frequencies.

Leg at right angle to flow field

Under these conditions velocity first peaks close to the cuticular surface and then decreases towards the value of v_∞ (figure 16). The distances of the velocity peaks from the leg surface are about 850 µm at 50 Hz, and about 650 µm at 150 Hz.

hair length. Only in tibial group LP such a correlation is found (figure 14). Among all 85 trichobothria examined there were 13 cases (15%) for $a < 0.5$, 53 cases (63%) for $0.5 < a < 1$, and 19 cases (22%) for $1 < a < 2$. The highest value found for a was 1.6.
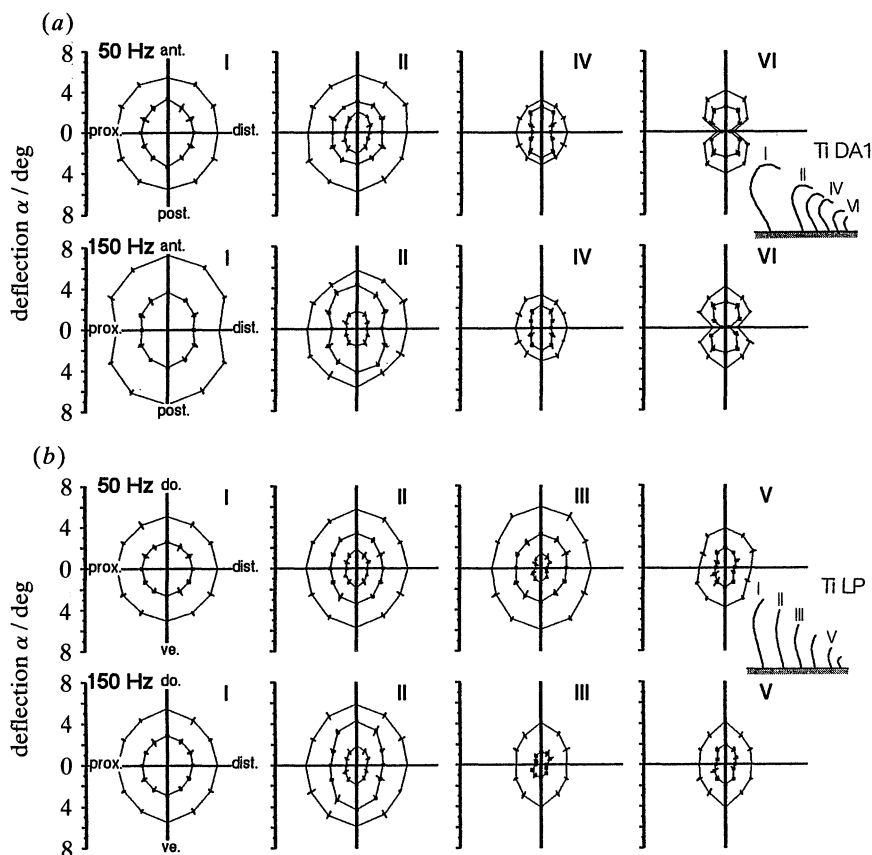

Figure 5. Mechanical directionality of hair deflection in oscillating air. Trichobothria of different lengths from tibial groups DA1 and LP tested at 50 Hz and 150 Hz and at different air particle velocities. (*a*) Group DA1 with hairs I (1250 µm), II (800 µm), IV (550 µm), and VI (350 µm). Particle velocities in mm s⁻¹ were as follows at 50 Hz (150 Hz): hair I, 12 and 29 mm s⁻¹ (27 and 59 mm s⁻¹); II, 12, 29 and 105 (8, 24, and 59); IV, 60 and 120 (19 and 51); VI, 69 and 150 (29 and 74). (*b*) Group LP with hairs I (1120 µm), II (1000 µm), III (700 µm), and V (450 µm). Particle velocities at 50 Hz (150 Hz): hair I, 16 and 40 mm s⁻¹ (29 and 53 mm s⁻¹); II, 21, 58 and 143 (16, 44 and 97); III, 17, 74 and 199 (9 and 44); V, 59 and 217 (26 and 86).
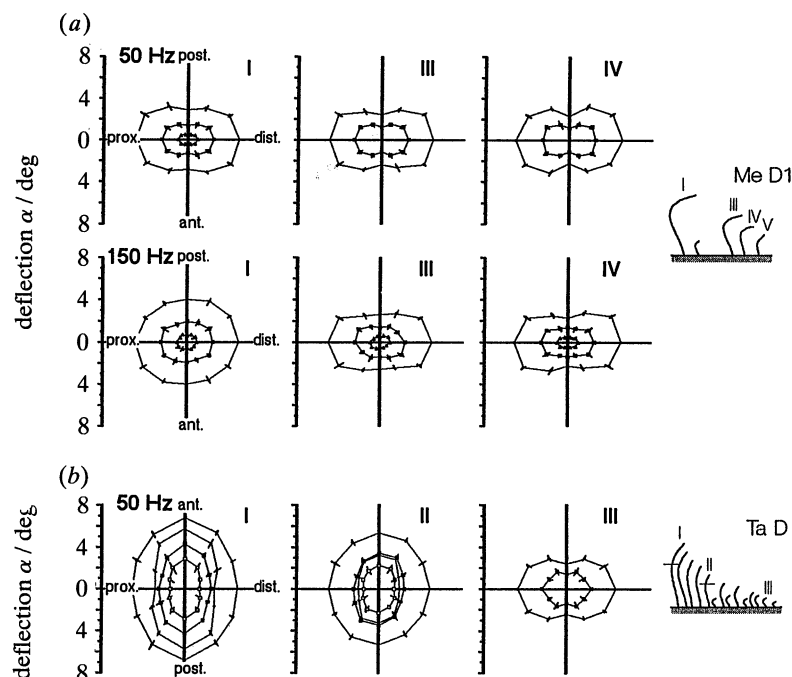
Figure 6. Mechanical directionality of hair deflection in oscillating air. Trichobothria of different length from metatarsal group D1 and tarsal group D tested at 50 Hz and 150 Hz. (a) Group MeD1 with hairs I (750 µm), III (600 µm), and IV (500 µm). Particle velocities in mm s^{-1} were the following at 50 Hz (150 Hz): hair I, 5, 16, and 24 mm s^{-1} (6, 15, and 31 mm s^{-1}); III, 12 and 30 (6, 12, and 29); IV, 12 and 34 (6, 12 and 27). (b) Group TaD with hairs I (900 µm), II (700 µm), and III (300 µm). Particle velocities at 50 Hz: hair I, 11 and 23; II, 13 and 19; III, 47 and 90. The innermost two curves (open circles) for hair I and hair II show directionality after cutting hairs at level shown in insert.

(b) Numerical

The experimentally measured data on the mechanical behaviour of the trichobothria in oscillating air flows were compared with equivalent data derived from the numerical analysis presented in the companion paper (Humphrey *et al.* 1993). Similarly,

analytical formulae for air velocity, also provided in that reference, were used to compare with present measurements. In general we find remarkably good agreement between all measurements and calculations.
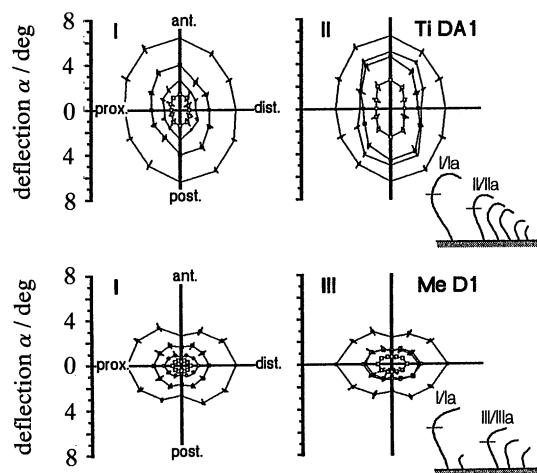

Figure 7. Effect of cutting distal curved part of hair. Directionality of hairs I (1000 µm) and II (750 µm) of tibial group DA1 and of hairs I (700 µm) and III (600 µm) of metatarsal group D1 was first examined in intact hairs (filled circles) and then after cutting off the hairs' distal bend (open circles) as shown in inserts. Oscillating frequency of air 50 Hz. Particle velocities in mm s^{-1} were the following: TiDA1: hair I, 17 and 31; II, 52 and 123; MeD1: hair I, 15 and 26; III, 13 and 27.
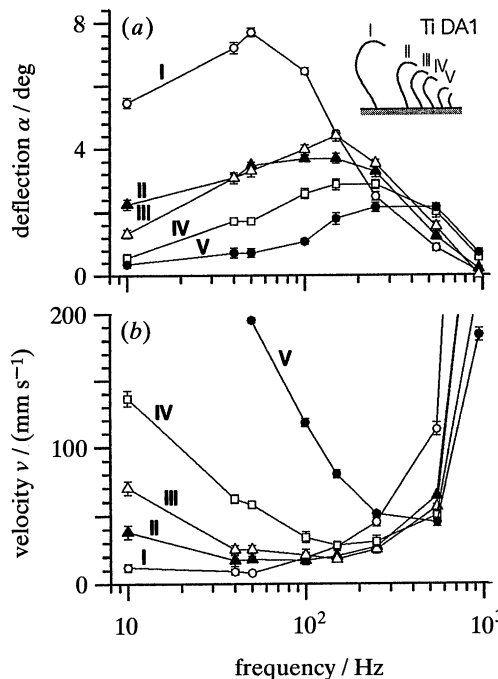

Figure 8. Tuning of trichobothria of tibial group DA1. Lengths of hairs I to V were 1150 µm, 700 µm, 650 µm, 500 µm, and 400 µm. (a) Deflection at constant particle velocity of 50 mm s^{-1}. (b) Air particle velocity necessary to get a constant hair deflection angle of 2.5°.
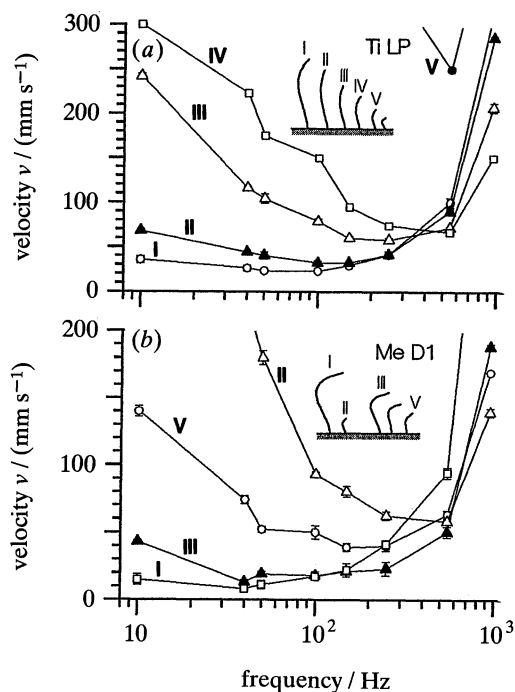
Figure 9. Tuning of trichobothria of tibial group LP and metatarsal group D1. Lengths of hairs I to V in group TiLP were 1150 μm, 1050 μm, 750 μm, 450 μm, and 300 μm. Trichobothria of group MeD1 were 850 μm (I), 200 μm (II), 500 μm (III), and 300 μm (V) long. Deflection angle of hairs kept constant at 2.5°.

(i) Airflow fields

Airflow velocity profiles were calculated for the conditions of figures 15 and 16 for the parallel and perpendicular substrate–airflow relative orientations,

respectively. The substrate (or leg) diameter was set to $D = 1.25$ mm. The rather close correspondence between the measured and calculated results for maximum velocity in an oscillation cycle (figures 15 and 16) confirms the ability of the analytical formulae to capture correctly: (i) the viscous damping of air motion near the substrate; (ii) the effect of substrate curvature on the air velocity which, in the perpendicular orientation, leads to a significant local acceleration of the flow immediately above the substrate; and (iii) the correct magnitude of the boundary layer thickness for both orientations.

(ii) Determination of R and S

As the phase shift between hair displacement and air velocity as a function of frequency is not known, the methodology described by Humphrey *et al.* (1993) to determine the damping constant R ($N\,m\,s\,rad^{-1}$) and the torsional restoring constant S ($N\,m\,rad^{-1}$) could not be employed for the trichobothria of this study. Instead, we obtained these two parameters by trial and error, by systematically comparing measured and calculated hair displacements as a function of frequency for different pairs of R and S. The parameters were determined for two hairs corresponding to the physical dimensions of a pair of hairs in the MeD1 cluster (figures 1 and 2) and characterized in terms of their displacement versus frequency in figure 11. One hair (I) was a long bent hair. The other hair (II) was a short straight hair. A substrate–airflow parallel orientation was assumed, in agreement with the experiment. The oscillating free stream velocity was set to the maximum value investigated experimentally, 50 mm s^{-1} and the substrate diameter was
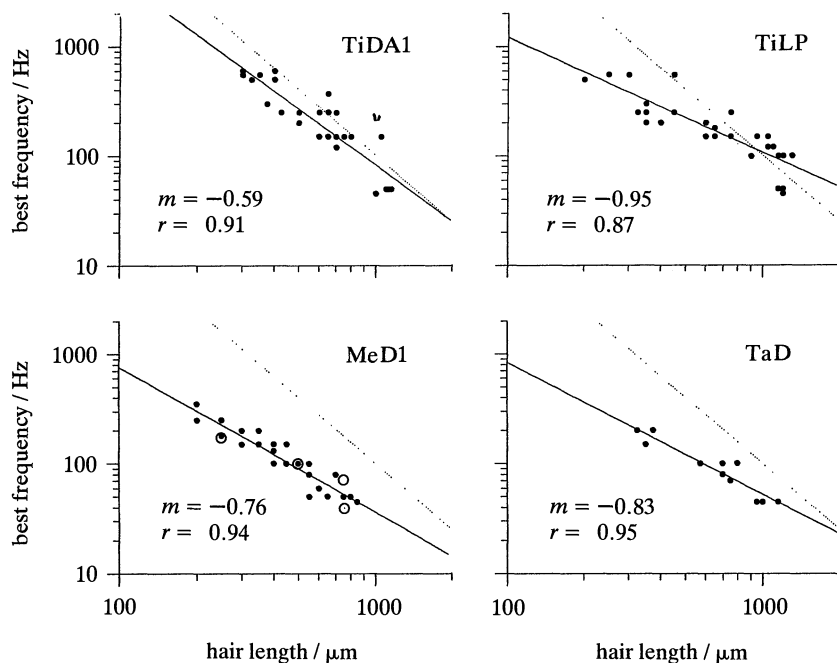

Figure 10. Best frequencies as a function of hair length. Open circles (MeD1) represent theoretical values derived from figure 19a; at 750 μm hair length the upper value represents a bent hair ($L_1 + L_2 = 750 + 250 = 1000$ μm), the lower value a straight hair ($L_1 = 750$ μm, $L_2 = 0$ μm). Dotted line corresponds to calculated boundary layer thickness (Stokes flow). r, correlation coefficient ($p > 0.005$ in all four cases); m refers to the relation $l \approx f^m$, i.e. it is the reciprocal value of the slope of the regression line in the figure. $n = 28, 33, 28$ and 11 for TiDA1, TiLP, MeD1, and TaD, respectively.
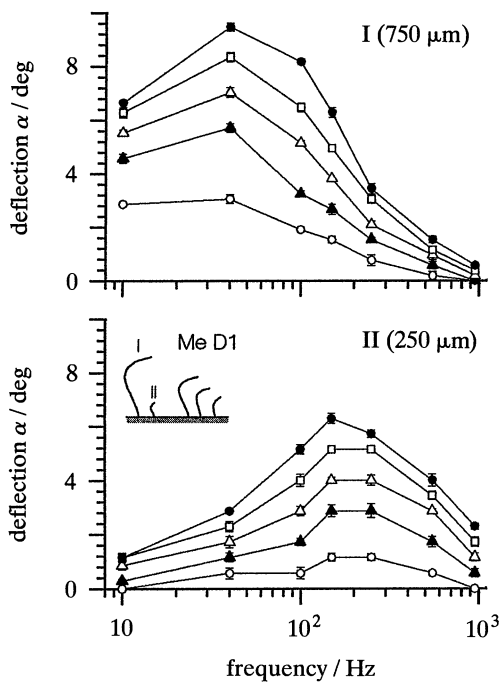
Figure 11. Tuning as a function of particle velocity. Hair deflection was measured at 10 (open circles), 20 (filled triangles), 30 (open triangles), 40 (open squares), and 50 (filled circles) mm s^{-1}. All values are averages of five measurements. Bars give s.d..
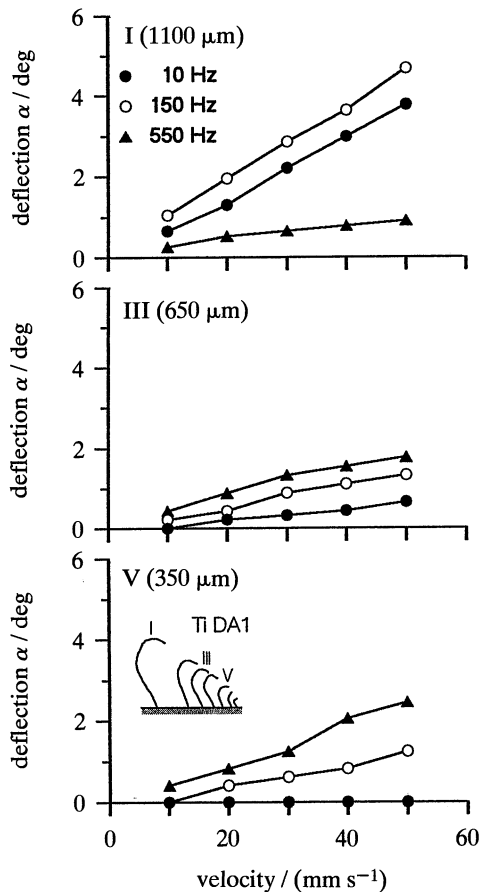

Figure 12. Deflection angle as a function of particle velocity. Three hairs of tibial group DA1 were examined at 10, 150, and 550 Hz.

fixed to $D = 1.25$ mm, the diameter of the spider leg at the location of the two hairs. The physical properties of air at 20°C were employed.

The best results calculated for hair displacement versus frequency correspond to $R = 2.20 \times 10^{-15}$ and $S = 5.77 \times 10^{-12}$ for the long hair and $R = 0.27 \times 10^{-15}$ and $S = 0.62 \times 10^{-12}$ for the short hair (figure 17). We note the much larger values of both parameters for the long hair. In general, agreement between the measurements and the calculations is quite good, especially with regard to the best frequency.

Given the differences that are bound to exist between the detailed distribution of velocity around the substrate in the experiment and that assumed for the calculations, it is impossible to determine the pair of (R,S) values which will yield values of hair deflection exactly matching the measurements. Notwithstanding, the agreement between the present values of S and those measured by Shimozawa & Kanou (1984) for the filiform hairs of crickets of similar dimensions to the present trichobothria is remarkable. For R we have no experimental data with which to compare. However, in Humphrey et al. (1993) we derived an approximate value for this parameter from the data of Kämper & Kleindienst (1990) for a filiform hair 1050 µm long and of diameter 5 µm. The result was $R = 2.22 \times 10^{-15}$ which is in excellent agreement with the value found here for the long (I) hair. With these values of R and S established, we were able to conduct calculations with confidence for other characteristics of hair motion.

(iii) *Solid versus hollow hairs*

The effect of 'hollowness' (i.e. mass) on hair motion was calculated for three straight hairs of lengths 500, 1000 and 1500 µm, respectively. In all cases an external diameter of 7 µm and an internal diameter of 3.5 µm were fixed. The pair of (R,S) values used was held constant to the values for the above long (I) hair. The amplitude of the far field velocity was taken as 50 mm s^{-1} for both parallel and perpendicular substrate–airflow orientations. The substrate diameter was $D = 1.25$ mm.

Figure 18 provides typical results for the 500 µm hair. Irrespective of frequency, for a fixed substrate–airflow orientation very small differences arise between the deflections of a solid hair and a hollow hair. For the longer hairs the differences were even smaller. We conclude that the dynamic characteristics of hair motion are essentially insensitive to the degree of hollowness of a hair, i.e. its mass. All subsequent calculations of hair motion were performed assuming solid hairs.

(iv) *Bent versus straight hairs*

The effect of hair shape (bent versus straight) on directionality was investigated by calculating the characteristics of a hair similar to hair I (uncut) and Ia (cut) of group MED1 in figure 7 for both the parallel and perpendicular flow orientations. The length of the cut hair was set equal to $L_1 = 750$ µm. For the uncut hair the straight portion was set to $L_1 = 750$ µm while the bent portion was set to
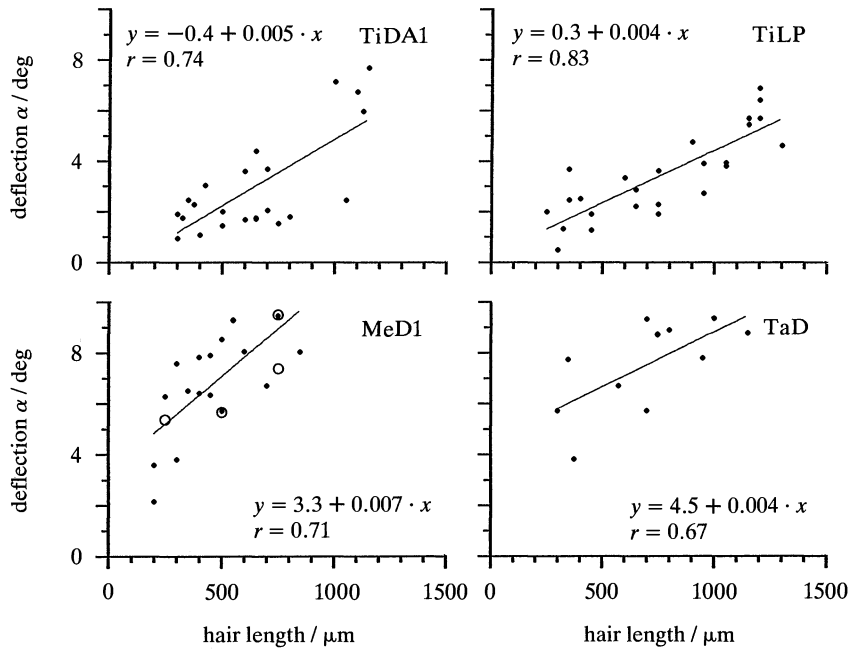
Figure 13. Deflection angle as a function of hair length. Hairs of four groups were examined at their individual best frequency and using a particle velocity of 50 mm s^{-1} for stimulation. Open circles represent theoretical values derived from figure 19a; at 750 µm hair length the lower value represents a bent hair ($L_1 + L_2 = 750 + 250 = 1000$ µm), the upper value a straight hair ($L_1 = 750$ µm, $L_2 = 0$ µm). r, correlation coefficient ($p < 0.005$ for TiDA1, TiLP, and MeD1 and $p < 0.05$ for TaD).

$L_2 = 250$ µm. In both cases the hair diameter was $d = 7$ µm. As in the experiments, the far field velocity was set to 26 mm s^{-1} at a flow oscillation frequency of $f = 50$ Hz. For both the cut and uncut hair the values of R and S were fixed to the values for the uncut hair (I): $R = 2.20 \times 10^{-15}$ and $S = 5.77 \times 10^{-12}$.

The ratios of maximum deflection (at the best frequency) of the hair in flow perpendicular to the
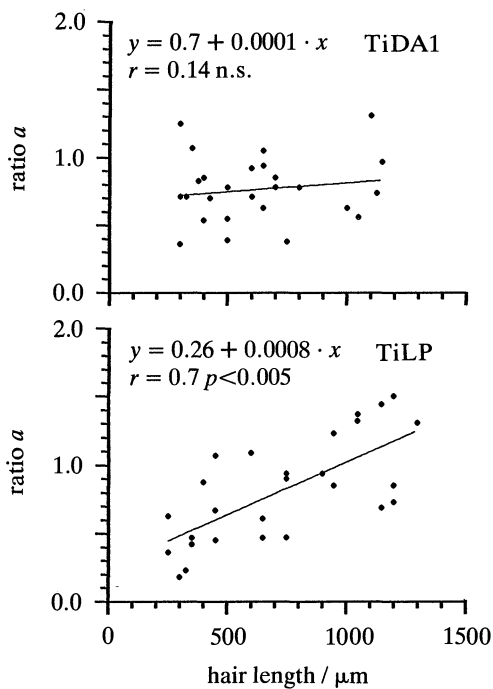

Figure 14. Ratio 'a' of hair tip deflection and air particle displacement. r, correlation coefficient; n.s., not significant; airflow parallel long leg axis.
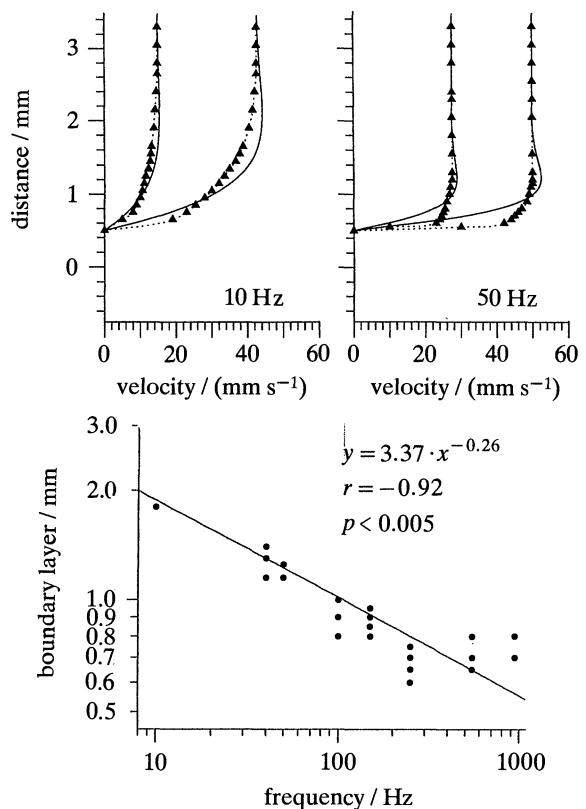

Figure 15. Velocity profiles and boundary layer. Top: measurements of profiles were taken above proximal, dorsal metatarsus at 10 Hz and 50 Hz, at two free field particle velocities (v_∞), and with the leg oriented parallel to the axis of the flow field. Triangles and dotted line represent measured values whereas the solid line is calculated according to Humphrey *et al.* (1993). Bottom: boundary layer thickness as a function of air oscillation frequency.
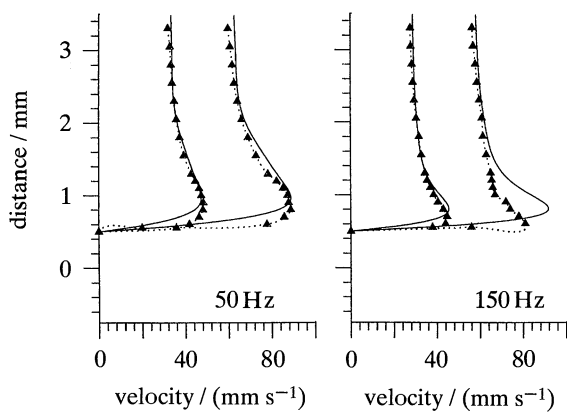
Figure 16. Velocity profiles. Same as in figure 15 but with leg oriented at right angle to axis of flow field.

longitudinal axis of the leg relative to its deflection in flow parallel to that axis were, approximately, $5.7°:3.8° = 1.5$ for the cut hair and $8.3°:5° = 1.7$ for the uncut hair. The closeness of these two ratios reinforces the experimental observation (figure 7) that the bend in a trichobothrium does not significantly influence its mechanical directionality which, therefore, must be due to the mechanical properties of the attachment of the hair to the substrate.

(v) *Tuning*

The above measurements and calculations show that the range of best frequency shifts to higher values
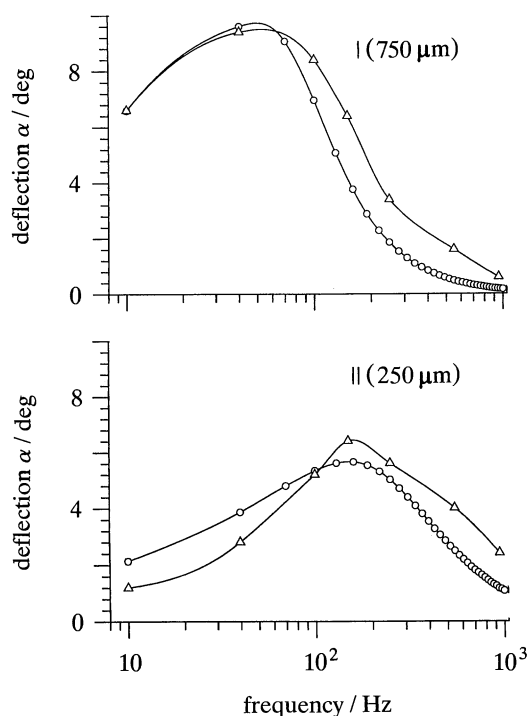

Figure 17. Determination of the damping constant R and of the torsional restoring constant S by matching calculated with measured values of hair deflection over frequency. Calculated values, open circles; measured values, open triangles. Measured values correspond to those in figure 11. For the calculated values the long hair was taken to have a straight portion (L_1) of 750 μm, a distal bent portion (L_2) of 250 μm, and a diameter (d) of 7 μm. For the short hair $L_1 = 250$ μm, $L_2 = 0$, and $d = 5$ μm. See text for more details.
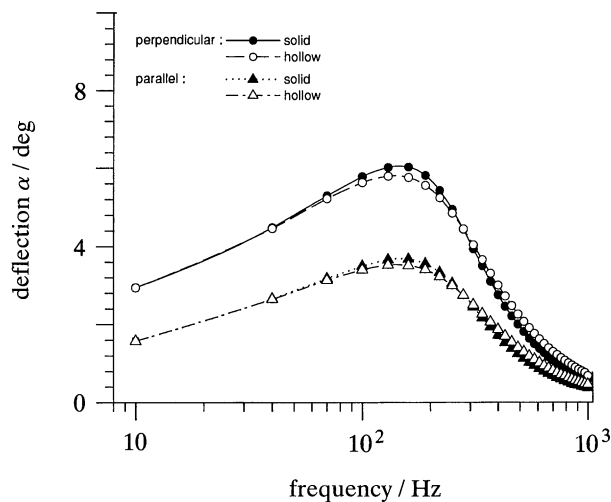

Figure 18. Calculation showing insensitivity of hair motion to changes in real mass of the hair. Deflection of hollow and solid hair are about the same, both in airflow parallel and perpendicular to the long leg axis. The hair modelled here is 500 μm long (L_1) and straight ($L_2 = 0$) with a diameter (d) of 7 μm.

for cut (shortened) hairs. To further investigate the effect of hair length on best frequency, calculations were performed for three straight hairs of lengths 250, 500 and 750 μm roughly corresponding to MeD1 hairs in figures 13 and 14. The values of R and S determined above were used for the shortest and longest hairs. For the intermediate, 500 μm, hair we used the averages of those results. For the hair diameters we took 5, 6, and 7 μm for increasing hair length. The amplitude of the oscillating free stream velocity was set to 50 mm s^{-1} for a substrate–airflow parallel orientation and the substrate diameter was fixed to 1.25 mm.

Results for hair displacement, velocity, acceleration and the ratio of hair tip displacement to free stream air element displacement are plotted in figure 19a–d. From the displacement profiles we determined the best frequencies as a function of hair length and plotted these results, as well as that shown for the long bent hair in figure 17, against the experimental measurements in figure 10. Similarly, calculated values for hair displacement at the best frequency are plotted against the measurements as a function of hair length in figure 13. In both cases the agreement between measurements and calculations is quite good.

The profiles for hair velocity versus frequency (figure 19b) display several remarkable features. First is the large range in frequency smoothly fractionated by the three hairs of different lengths. For example, where the frequency sensitivity of the 750 μm hair peaks (the maximum velocity at 130 Hz, approximately) that of the shorter hairs shows the highest sensitivity to frequency change (steepest slope). Second is that this phenomenon is peculiar to each hair and for it to occur two conditions are required. These are that: (i) $R_t^2 < 2I_t S$; and (ii) $S_1/S_2 > I_{t1}/I_{t2}$. In these expressions R_t, I_t and S are, respectively, the total damping constant, total moment of inertia and torsional restoring constant of any hair (Humph-

rey *et al*. 1993). When subscribed '1' and '2' they refer to specific hairs. Although algebraically involved to derive, the conditions follow from the inviscid flow analysis presented in Appendix 1 of Humphrey *et al*. (1993). Third is the observation that the value of frequency at which this phenomenon takes place on the velocity figure (in the present case for the 750 μm hair) coincides exactly with the frequency at which hair displacement performance crosses over in figure 19*a*.

In contrast to velocity, the curves for hair acceleration versus frequency (figure 19*c*) reveal a relative insensitivity of hair length to frequency changes in the range 10 to 150 Hz. Above 150 Hz these profiles start deviating significantly (linearly on the semi-log plot) with slopes inversely proportional to hair length.

(vi) *Optimal hair length*

Neither the measurements nor the calculations in figure 10 support the statements by Fletcher (1978) and Tautz (1979) that hair length varies with best frequency according to $L \approx f^{-1/2}$. A comparison between the best frequencies for hair deflection (figure 19*a*) and best frequencies for the ratio *a*, the maximum hair tip displacement to air element displacement plotted in figure 19*d*, shows that for a given hair length the two do not coincide. That this must be the case is demonstrated by noting that $\alpha = f(\omega)$, while ratio $a = (\omega/U_o) f(\omega)$, where U_o is the amplitude of the free stream velocity. It is easy to show that the respective best frequencies for α and ratio *a* cannot possibly coincide unless $f(\omega) = 0$, and this is not the case. In addition, it is clear from the hair displacement and ratio *a* profiles that, for a given hair length, the maximum value of the ratio *a* is attained with a hair deflection smaller than the maximum hair deflection at the best frequency. Finally, we note that the maximum ratio *a* calculated does not exceed 1.25, which is considerably less than the limit of 2 proposed by Fletcher (1978) and Tautz (1979) on the basis of an inviscid flow analysis for air oscillating over a flat substrate. The measured values of the ratio *a* (figure 14) in most cases (78%) were smaller than 1.0. The highest value ever found was 1.6. In the case of group MeD1, which was also chosen for the numerical analysis, the largest measured value for ratio *a* was 1.1.

From figure 19*d* we find that the best frequencies for the ratio *a* of the hairs 750, 500 and 250 μm long are 130, 220 and 400 Hz, respectively. The best frequencies determined from hair deflection measurements (figure 10, MeD1) were about 50, 200 and 300 Hz, i.e. closer to the calculated values in figure 19*a* than those in figure 19*d*, as expected. Using the ratio *a* as an appropriate measure for hair mechanical sensitivity to airflow oscillations, these frequencies will then correspond to values to which these hairs are, respectively, most sensitive and for which, we argue, they have been optimally designed.

Since the Stokes flow boundary layer thickness, δ, varies according to $\delta = 6.5 \ (v/2\pi f)^{1/2}$ (v, kinematic viscosity of air), we find the following approximate correspondence between hair length and boundary
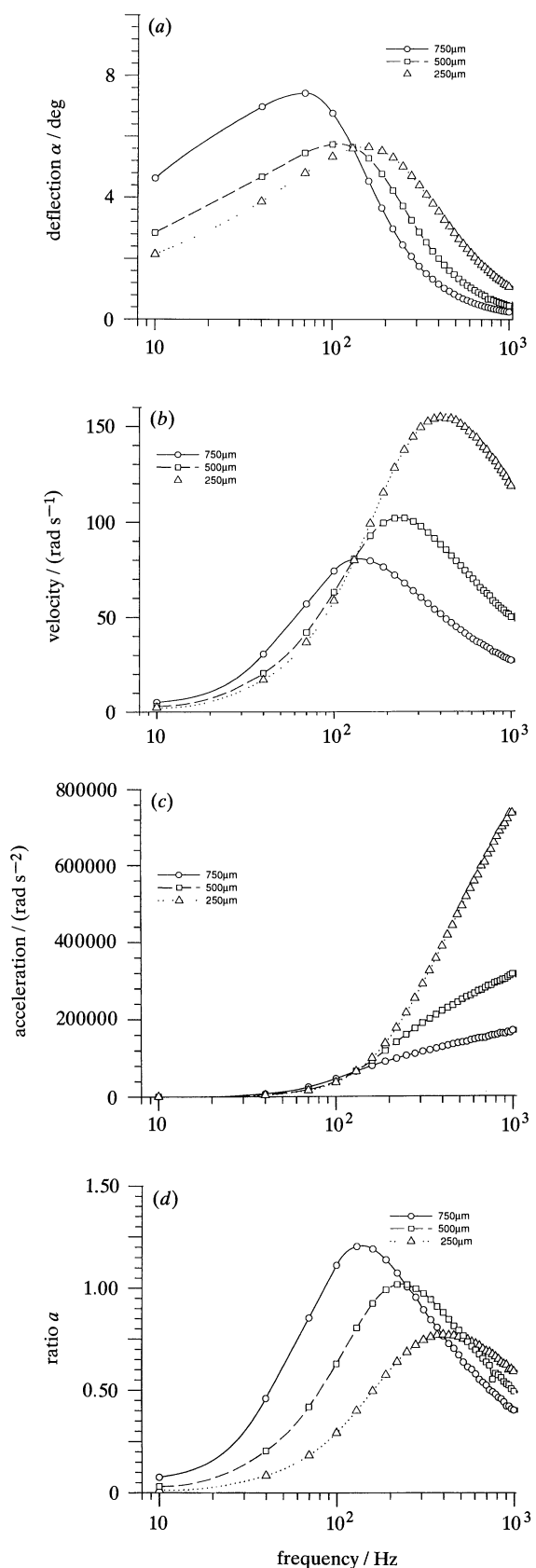

Figure 19. Dependence of hair deflection, velocity, and acceleration on the frequency of the oscillating airflow. Calculations were performed for straight hairs ($L_2 = 0$) of lengths (L_1) 250, 500, and 750 μm and diameters (d) 5, 6 and 7 μm. For a comparison of calculated values in figure 19*a* with measured values see figures 10 and 13. In figure 19*d* ratio *a* (maximum hairtip displacement:air particle displacement) is given as a function of airflow frequency.

layer thickness: $L_1 = 750$ μm, $\delta = 865$ μm; $L_1 = 500$ μm, $\delta = 665$ μm; and, $L_1 = 250$ μm, $\delta = 493$ μm. If instead, as in Tautz (1979), we now associate the length of a hair with its best frequency and claim that it was designed to detect that frequency optimally, the same procedure yields the following hair length–boundary layer thickness pairs: $L_1 = 750$ μm, $\delta = 1178$ μm; $L_1 = 500$ μm, $\delta = 986$ μm; and $L_1 = 250$ μm, $\delta = 779$ μm.

4. DISCUSSION

(a) *Number and arrangement*

Adults of *Cupiennius salei* have about 100 trichobothria on each of their legs. This is by far the largest number recorded for a spider and suggests a particular behavioural significance of air movement detection in this species. Hunting spiders of smaller size such as *Philodromus aureolus* and *Pardosa prativaga* have only 21–23 and 37 trichobothria (Peters & Pfreundt 1986). *Agelena labyrinthica*, which hunts on a mechanically rather solid sheet web, has only about 25 as well (Reißland & Görner 1985; Görner & Andrews 1965).

However, the number of trichobothria seems not to depend solely on spider size. According to present knowledge an interesting general difference exists between hunting spiders and orb weavers as well as Linyphiidae. The latter two groups were found to have considerably fewer trichobothria than the hunting spiders. Examples are *Araneus cornutus*, *Meta reticulata*, and *Linyphia triangularis* all of which have only from seven to 11 trichobothria on a leg (Peters & Pfreundt 1986). *Nephila clavipes*, one of the largest orb weavers approaching *C. salei* in size, has about 40 trichobothria per leg (F. G. Barth, unpublished observations). According to the trichobothrial patterns established for phylogenetic purposes by Lehtinen (1980) *Cupiennius* is closest to the Amaurobiomorpha-type. *Nephila* belongs to the Araneomorpha-type which is close to the plesiomorphic pattern consisting of one metatarsal trichobothrium and two rows of tibial trichobothria but no trichobothria on the tarsus or femur.

Apart from differences in number there are differences in arrangement, the most obvious being the complete lack of trichobothria on the tarsus of the web spiders and the presence of only one or a very few on their metatarsus. With the available knowledge it is hard to interpret these differences functionally. Nevertheless, a few points should be raised. (i) The accumulation of trichobothria dorsally on the tarsus of hunting spiders may be related to the increase of flow velocity above a solid surface such as the plant leaves *C. salei* is usually sitting on relative to the situation in an orb web (Barth *et al.* 1988, unpublished data). Hairs on the tarsus may thus be positioned in a particularly 'sensitive' area of the stimulus field. This idea is supported by the lack of tarsal trichobothria in orb weavers sitting in a web largely transparent to the airflow. It should also be remembered that in a hunting spider it will always be a tarsus which sees an approaching stimulus first (except when it comes from directly above). (ii) The difference in number of

trichobothria between hunting spiders and orb weavers may be related to earlier observations (Klärner & Barth 1982) demonstrating the necessity of prey produced thread vibrations to elicit prey capture and the ineffectiveness of air movement stimuli (such as that of an insect in flight) which elicit defensive raising of the front legs. The latter behaviour seems to ask for less precision in oriented movement and spatial analysis of the stimulus field than does prey capture. (iii) The trichobothria may have evolved dorsally to detect air motion generally directed to the spider from above it.

(b) *Hair structure*

The most obvious features of the trichobothrial hair shafts in *C. salei* are their sculptured, feathery surface, the tip curvature seen in many of them, and differences in length.

1. The delicate *surface structures* point to an optimization of hair design for two reasons. First, they increase the drag exerted by the moving air relative to a corresponding smoother cylindrical surface thus enhancing the mechanical sensitivity of the hair. They do this by arresting the motion of air in the spaces between the structures forming the fine branches, thus increasing the effective diameter of the hair seen by the flow. There are two reasons for this. The flow around a trichobothrium at Reynolds numbers of about 10^{-2} is dominated by viscous forces. In addition, the distance between individual branches is very small; we counted from four to 14 of them within 10 μm along a line parallel to the hair's long axis. Viscous forces acting on the air located between and above the feathery branches will essentially stop any air movement in the spaces between the branches (Schlichting 1979).

Second, the breaking up of a solid volume into a feathery structure adds considerably to the light weight 'design' of the hair. Regarding inertial mass (as opposed to drag) the relevant diameter of the hair lies between the inner diameter of the shaft supporting the structures and the outer diameter defined by the edges of the structures. The latter of these two quantities is taken as the effective diameter of the hair for calculating drag.

A feathery surface is also known of the trichobothria of other species of spiders (Görner 1965; Harris & Mill 1977). It is not a rule for filiform hairs in general, however. There are spider (e.g. *Nephila clavipes*; F. G. Barth unpublished observations), scorpion (Messlinger 1987), and insect filiform hairs (Shimozawa & Kanou 1984*a*) with a rather smooth surface. Regarding the effect on inertial forces, theory (Fletcher 1978; Humphrey *et al.* 1993) indeed predicts only a minor effect of mass reduction as is demonstrated by a comparison of the motion of hollow and solid hairs, respectively (figure 8).

2. *Curvature* of the trichobothrial hair shafts was initially hypothesized by us to lead to mechanical directionality, i.e. an increased deflection by air currents oriented at right angle to the plane of the hair. According to our experiments this assumption is

wrong. The directional properties remain the same after cutting the curved part of the hair. Because, in addition, it is some of the very short and straight hairs which exhibit the most pronounced mechanical directionality we conclude that directionality resides in the hair's articulation or the structures coupling it to the dendrites. Neither the trichobothria of other arachnids (Palmgren 1936; Hoffmann 1967; Görner & Andrews 1969; Harris & Mill 1977; Peters & Pfreundt 1986; Meßlinger 1987) nor the filiform hairs of insects (Nicklaus 1965; Shimozawa & Kanou 1984a; Gnatzy & Tautz 1980) are curved like the trichobothria of *Cupiennius salei*. The only case known to us are four filiform hairs on the first thoracal segment of a caterpillar. These hairs do indeed show the expected mechanical directionality (Tautz 1977). In this case then, the mechanics of the hair's articulation either does not dominate the directionality of the hair or has the same effect on it as the bend of the hair.

We speculate that an important functional consequence of the curvature of trichobothria located dorsally on the leg of *C. salei* is an enhancement of their mechanical sensitivity to air movement from above. This certainly is a common stimulus situation in which the drag forces induced yield a net component that can make the hair oscillate.

3. Differences in *length* are in similar ranges in the trichobothria of *C. salei* (100–1400 μm) and indeed of *Euscorpius carpathicus* (550–1050 μm; Hoffmann 1967) and in insect filiform hairs (*Barathra* caterpillar 450–650 μm, Tautz 1977; *Gryllus bimaculatus* 30–1500 μm, Shimozawa & Kanou 1984a; *Locusta migratoria* 20–500 μm, Boyan *et al.* 1989). Clusters of sensilla with a regular arrangement of increasing hair lengths are only known for spider trichobothria (see also Palmgren 1936; Görner & Andrews 1969; Harris & Mill 1977; Peters & Pfreundt 1986). Differences in trichobothrial hair length go along with differences in absolute mechanical sensitivity which increases with hair length as is most readily seen from our experiments with cut hairs. This implies that they provide for a fractionation of a large range of mechanical sensitivity. In case of the clusters formed by spider trichobothria this amounts to the availability of a spatially concentrated analysis of a wide range of stimulus amplitudes. To test the biological significance of absolute sensitivity in *Cupiennius salei* we recently measured the sensory space accessible to the trichobothria. A fly humming in a fixed position elicits prey capture behaviour at distances up to about 30 cm and induces trichobothrial deflection at distances up to about 60 cm (Barth *et al.* 1993). This contrasts with findings in *Agelena* and *Tegenaria* where the equivalent value for prey capture was given as about 1 cm by Reißland & Görner (1978) and is instead much closer to values given for the *Barathra* caterpillar by Tautz (1977). In this regard, application of the term 'touch at a distance' used by Reißland & Görner to describe the function of the spider trichobothrial system would be misleading in case of *Cupiennius*. According to our direct measurement of boundary layer thickness, differences in hair length are also a basis for frequency discrimination on fluid mechanical grounds. Bound-

ary layer thicknesses at frequencies of biological interest fall well within the range of trichobothria length. Although broad, the tuning of the hairs significantly changes with hair length. Our results do not agree with the conclusion of Reißland & Görner (1978) made for agelenid spiders, that there is no mechanical basis for frequency discrimination by the trichobothria. Our data instead support the notion (Fletcher 1978; Tautz 1979; Shimozawa & Kanou 1984b; Humphrey *et al.* 1993) of mechanical filters transforming frequency-dependent velocity profiles (boundary layers) into hair deflection with the range of best frequencies depending on hair length. The tuning of the trichobothria can thus only be understood by considering details of the airflow around them.

Following Fletcher (1978) and Tautz (1979) a judgement of mechanical sensitivity of a hair can be based on a comparison of hair tip displacement and air particle displacement. We correlated ratio *a* of hair tip displacement and air particle displacement for 85 hairs at their best frequency. There was considerable variation within a size class and no significant correlation in three of the four trichobothrial groups examined. The exception was group LP on the tibia. Similar to findings in cricket filiform hairs (Kämper & Kleindienst 1990) *a* assumed values between 0.18 and 1.6 but never 2, the value predicted on theoretical grounds for an ideal hairlike movement detector (Fletcher 1978; Tautz 1979). Only in 22% of the cases hairtip displacement exceeded air particle displacement. Humphrey *et al.* (1993) show that if a 2π error in Fletcher's (1978) analysis is accounted for the maximum ratio *a* predicted by that analysis is 1.5 as opposed to 2.

In earlier work (Shimozawa & Kanou 1984a,b) it has been argued that short hairs are primarily acceleration sensitive and long ones velocity sensitive. From our findings we conclude that when all contributions to the torque balance are included in the equation of motion for the hair and proper values are provided for the hair parameters, R and S, as a function of hair length, short hairs are as good or better velocity sensors as long hairs, and are superior acceleration sensors.

As argued by Fletcher and Tautz, the length of an optimally adapted hair should be between about two and six times the boundary layer thickness. The latter changes with frequency of oscillation and on the basis of this Tautz (1979) calculated the frequency ranges to which hairs of a particular length should be best adapted. In short, the length of a hair should be roughly inversely proportional to the square root of the frequency it is designed to detect, provided boundary layer thickness $\delta = 6.5\sqrt{(\nu/2\pi f)}$ (flat infinite plate). From our figure 10 it can be seen that most hairs have lengths smaller than δ (see below on optimal hair length). Theoretical best frequency values derived for group MeD1 from figure 19a show good agreement with the values determined experimentally.

4. The bilateral symmetry in the structure of the cup surrounding the base of a trichobothrium of

Cupiennius salei is similar to that already known for other spiders (Görner 1965; Harris & Mill 1977). It contrasts with the radial symmetry of the cup of both scorpion trichobothria (Hoffmann 1967; Messlinger 1987) and insect filiform hairs (Gnatzy & Tautz 1980; Shimozawa & Kanou 1984a; Boyan *et al.* 1989). Nevertheless, directional properties of hair deflection in *Cupiennius* cannot be related to cup structure but are attributed to properties of the hair's articulation as in case of insect filiform hairs (Gnatzy & Tautz 1980).

Maximum deflection of a hair (before it touches the cup) is very large in *Cupiennius*. It amounts to 25° to 35° as compared to about 5° in the cricket (Gnatzy & Tautz 1980; Kämper & Kleindienst 1990). This difference indicates a much larger working range of the spider trichobothria than of the filiform hairs of these insects and may be related to the respective behaviours guided by them. Whereas the insect filiform hairs are closely linked to the triggering of a quick escape response to the slightest movement of air (Roeder 1963; Camhi *et al.* 1978) *Cupiennius* is using its trichobothria to identify and orient towards prey signals which may contain airflow velocities as big as $0.7 \, \mathrm{m \, s^{-1}}$ and more (Barth *et al.* 1993). The larger range of best frequencies shown in the present study for *Cupiennius* (*ca.* 50–600 Hz) as compared to the cricket filiform hairs (*ca.* 40–100 Hz; Kämper & Kleindienst 1990) may have to be interpreted along the same line of argument.

(c) Directionality

Insect filiform hairs are supplied by a single sensory cell and typically exhibit a pronounced mechanical directional sensitivity. Spider trichobothria typically do not exhibit such mechanical directionality. They are supplied by three or four sensory cells (four in *Cupiennius*; Anton & Barth 1992). These are in turn activated when the hair is deflected in particular directional ranges specific to the individual cell. Thus, whereas in the case of insects it is the hair that 'looks' in a particular direction, it is the sensory cells in the case of spiders (Görner 1965; Nicklaus 1965, 1967; Gnatzy & Tautz 1980; Reißland & Görner 1978; K. Zapfel & F. G. Barth, unpublished data). Our own data for *C. salei* only partly confirm the mechanical isotropy of spider trichobothria. Although there are cases of hairs with perfect mechanical isotropy, in others the directionality plots form ellipsoids, and, in a few cases, cardioids are even formed. The latter is particularly obvious in the very short hairs. The bend so characteristic of the majority of hairs is not related to this difference, nor is the opening of the cup whose axis of bilateral symmetry is oriented parallel to the long leg axis in all cases. Since neither hair curvature nor the cup structure can be made responsible for the directionality of the trichobothria this is likely to reside in the spring supporting the hair at its base. Kanou *et al.* (1989) have recently verified this for cricket cercal hairs by quantitative measurements. Polarization factors were 4 to 8 in hairs 100–1000 μm long and spring stiffness increased in proportion to

the square power of hair length approximately. The absolute values were *ca.* 10^{10} to $10^{12} \, \mathrm{N \, m \, rad^{-1}}$.

(d) Velocity profiles and boundary layer

The region of slow-moving air very near the surface of the exoskeleton, referred to as the boundary layer, has been discussed with regard to hair motion by Fletcher (1978) and Tautz (1979). Shimozawa & Kanou (1984b) treated the underlying theoretical problems in some detail. These studies have been critically reviewed and extended in the companion paper by Humphrey *et al.* (1993). The present study provides the first actual measurements of such boundary layers. Despite the technical problems arising because of the small size of the LDA's measuring volume (§ 2) our data show that the boundary layers to be expected between 10 Hz and 950 Hz range between about 2600 μm and 600 μm. There is considerable overlap with the length distribution of the trichobothria (100–1400 μm) which underlines the significance of accounting for velocity variations through the boundary layer. In particular, our measurements of the velocity profiles of airflow at right angle to the long leg axis emphasize the importance of accounting for the influence of the curved surfaces of the cuticular structures carrying hairs on hair motion. The increase of velocity above the surface compared with v_∞ is considerable and at a distance (600–900 μm) well within the range of the trichobothria (or insect filiform hairs). When comparing boundary layer thickness calculated for an infinite flat plate as $\delta = 6.5\sqrt{(v/2\pi f)}$ (v, kinematic viscosity of air) (Schlichting 1979) with the values measured for airflow parallel to the long leg axis it is found that the latter are smaller at frequencies less than *ca.* 100 Hz and larger at frequencies greater than *ca.* 250 Hz. Thus, δ measured was *ca.* 2300 μm and 700 μm at 10 Hz and 950 μHz, respectively, whereas the corresponding calculated values are 3178 μm and 325 μm.

The conditions of hair motion chosen to calculate the relation between boundary layer thickness (Stokes flow) and hair length are very likely to trigger action potentials (Reißland & Görner 1985). Therefore we must conclude that the optimum length of a hair is no longer than the boundary layer thickness, δ. This finding might appear to contradict the earlier suggestion by Tautz (1979), based on Fletcher's (1978) work, that optimal hair length varies between 2δ and 6δ. Tautz's (1979) calculations of δ are based on an equation (Eq. (6) in his paper) that underpredicts δ by a factor of 6.5, approximately. The constant 6.5 is necessary to fix the location of the boundary layer at a distance from the substrate where velocity variations are 1% or less relative to the free stream value (Panton 1984). If allowance is made for this constant, the correct limits implied by Tautz's (1979) analysis are $0.3\delta \leqslant L_1 \leqslant 0.9\delta$, in good agreement with the range of values found above.

Regressions of the above calculated $L_1 - \delta$ pairs according to an expression of the form $L_1 \approx f^{-m}$ yields $m = 1.0$ ($r = 0.99$) when the boundary layer thickness measure is based on the best frequency for the ratio a,

and $m = 1.34$ ($r = 0.99$) when it is based on the best frequency of hair deflection. Both of these values are significantly larger in absolute terms than the value $m = 0.5$ proposed by Fletcher (1978) and Tautz (1979).

REFERENCES

Anton, S. & Barth, F.G. 1993 Central nervous projection pattern of trichobothria and other cuticular sensilla in the wandering spider *Cupiennius salei* Keys. *Zoomorphology* (In the press.)

Barth, F.G., Seyfarth, E.-A., Bleckmann, H. & Schüch W. 1988 Spiders of the genus *Cupiennius* Simon 1891 (Araneae, Ctenidae). I. Range distribution, dwelling plants and climatic characteristics of the habitats. *Oecologia* **77**, 187–193.

Barth, F.G., Wastl, U. & Humphrey, J.A.C. 1993 Dynamics of arthropod filiform hairs. III. Natural stimuli. (In preparation.)

Boyan, G.S., Williams, J.L.D & Ball, E.E. 1989 The wind-sensitive cercal receptor/giant interneurone system of the locust, *Locusta migratoria*. I. Anatomy of the system. *J. comp. Physiol.* A **165**, 495–510.

Camhi, J.M., Tom, W. & Volman, S. 1978 The escape behaviour of the cockroach *Periplaneta americana*. II Detection of natural predators by air displacement. *J. comp. Physiol.* **128**, 203–212.

Fletcher, N.H. 1978 Acoustical response of hair receptors in insects. *J. comp. Physiol.* **127**, 185–189.

Gnatzy, W. & Tautz, J. 1980 Ultrastructure and mechanical properties of an insect mechanoreceptor: stimulus-transmitting structures and sensory apparatus of the cercal filiform hairs of *Gryllus*. *Cell Tissue Res.* **213**, 441–463.

Görner, P. 1965 A proposed transducing mechanism for a multiply-innervated mechanoreceptor (trichobothrium) in spiders. *Cold Spring Harb. Symp. quant. Biol.* **30**, 69–73.

Görner, P. & Andrews, P. 1969 Trichobothrien, ein Ferntastsinnesorgan bei Webespinnen (Araneen). *Z. vergl. Physiol.* **64**, 301–317.

Harris, D.J. & Mill, P.J. 1977 Observations on the leg receptors of *Ciniflo* (Araneidae: Dictynidae) I. External Mechanoreceptors. *J. comp. Physiol.* **119**, 37–54.

Hoffmann, Ch. 1967 Bau und Funktion der Trichobothrien von *Euscorpius carpathicus* L. *Z. vergl. Physiol.* **54**, 290–352.

Humphrey, J.A.C., Devarakonda, R., Iglesias, J. & Barth, F.G. 1993 Dynamics of arthropod filiform hairs. I. Mathematical modelling of the hair and air motions. *Phil. Trans. R. Soc. Lond.* B **340**, 423–444. (Preceding paper.)

Kanou, M., Osawa, T. & Shimozawa, T. 1989 Mechanical polarization in the air-current sensory hair of a cricket. *Experientia* **45**, 1082–1083.

Kämper, G. & Kleindienst, H.U. 1990 Oscillation of cricket sensory hairs in a low-frequency sound field. *J. comp. Physiol.* A **167**, 193–200.

Klärner, C. & Barth, F.G. 1982 Vibratory signals and prey capture in orb-weaving spiders (*Zygiella x-notata*, *Nephila clavipes*; Araneidae). *J. comp. Physiol.* **148**, 445–455.

Lachmuth, U., Grasshoff, M. & Barth, F.G. 1984 Taxonomische Revision der Gattung *Cupiennius* Simon 1891 (Arachnida; Araneae). *Senckenbergiana biol.* **65**, 329–372.

Lehtinen, P.T. 1980 Trichobothrial patterns in high level taxonomy of spiders. *Proc. 8th International Conf. Arachnology*. Egermann Wien, 493–498.

Messlinger, K. 1987 Fine structure of scorpion trichobothria (Arachnida, Scorpiones). *Zoomorphology* **107**, 49–57.

Nicklaus, R. 1965 Die Erregung einzelner Fadenhaare von *Periplaneta americana* in Abhängigkeit von der Größe und Richtung der Auslenkung. *Z. vergl. Physiol.* **50**, 331–362.

Nicklaus, R. 1967 Zur Richtcharakteristik der Fadenhaare von *Periplaneta americana*. *Z. vergl. Physiol.* **54**, 434–437.

Palmgren, P. 1936 Experimentelle Untersuchungen über die Funktion der Trichobothrien bei *Tegenaria derhami* Scop. *Acta. Zool. Fenn.* **19**, 3–27.

Panton, R.L. 1984 *Incompressible flow*. New York: John Wiley and Sons.

Peters, W. & Pfreundt, C. 1986 Die Verteilung von Trichobothrien und lyraförmigen Organen an den Laufbeinen von Spinnen mit unterschiedlicher Lebensweise. *Zool. Beitr. N. F.* **29**, 209–225.

Prandtl, L. & Tietjens, H. 1934 *Applied hydro- & aeromechanics*. New York: Dover Publ. Inc.

Reißland, A. & Görner, P. 1978 Mechanics of trichobothria in orb-weaving spiders (*Agelenidae*, Araneae). *J. Comp. Physiol.* **123**, 59–69.

Reißland, A. & Görner, P. 1985 Trichobothria. In *Neurobiology of arachnids* (ed. F. G. Barth), pp. 138–161. Berlin, Heidelberg, New York and Tokyo: Springer.

Roeder, K. 1963 Evasive behavior in the cockroach. In *Nerve cells and insect behavior* (K. D. Roeder), pp. 71–88. Cambridge, Massachusetts: Harvard University Press.

Schlichting, H. 1979 *Boundary layer theory*. New York: McGraw-Hill.

Shimozawa, T. & Kanou, M. 1984a Varieties of filiform hairs: range fractionation by sensory afferents and cercal interneurons of a cricket. *J. comp. Physiol.* A **155**, 485–493.

Shimozawa, T. & Kanou, M. 1984b The aerodynamics and sensory physiology of range fractionation in the cercal filiform sensilla of the cricket *Gryllus bimaculatus*. *J. comp. Physiol.* A **155**, 495–505.

Tautz, J. 1977 Reception of medium vibration by thoracal hairs of caterpillars of *Barathra brassicae* L (Lepidoptera, Noctuidae). I. Mechanical properties of the receptor hairs. *J. comp. Physiol.* **118**, 13–31.

Tautz, J. 1978 Reception of medium vibration by thoracal hairs of caterpillars of *Barathra brassicae* L (Lepidoptera, Noctuidae). II. Response characteristics of the sensory cell. *J. comp. Physiol.* **125**, 67–77.

Tautz, J. 1979 Reception of particle oscillation in a medium – an unorthodox sensory capacity. *Naturwissenschaften* **66**, 452–461.
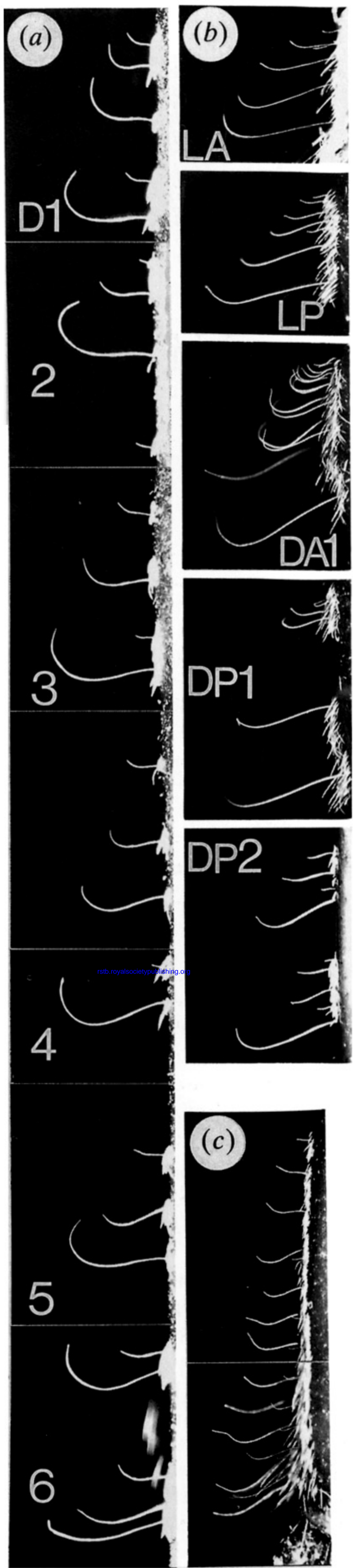
Figure 2. Trichobothria on walking leg. For abbreviations
see figure 1; (a) metatarsus, (b) tibia, (c) tarsus. Magnifica-
tion ×16.

(b)

$n = 107$
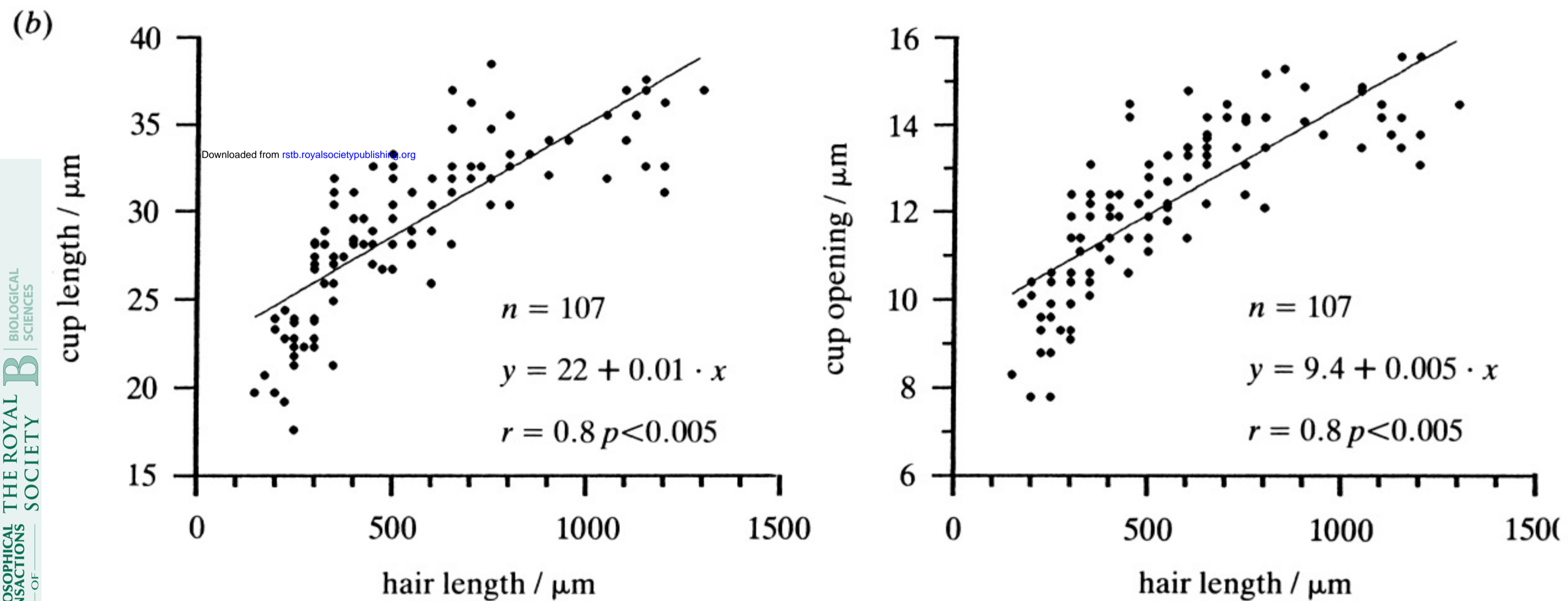
$y = 22 + 0.01 \cdot x$

$r = 0.8 \, p < 0.005$

$n = 107$

$y = 9.4 + 0.005 \cdot x$

$r = 0.8 \, p < 0.005$

(c)

4 μm

7 – 9 μm

α
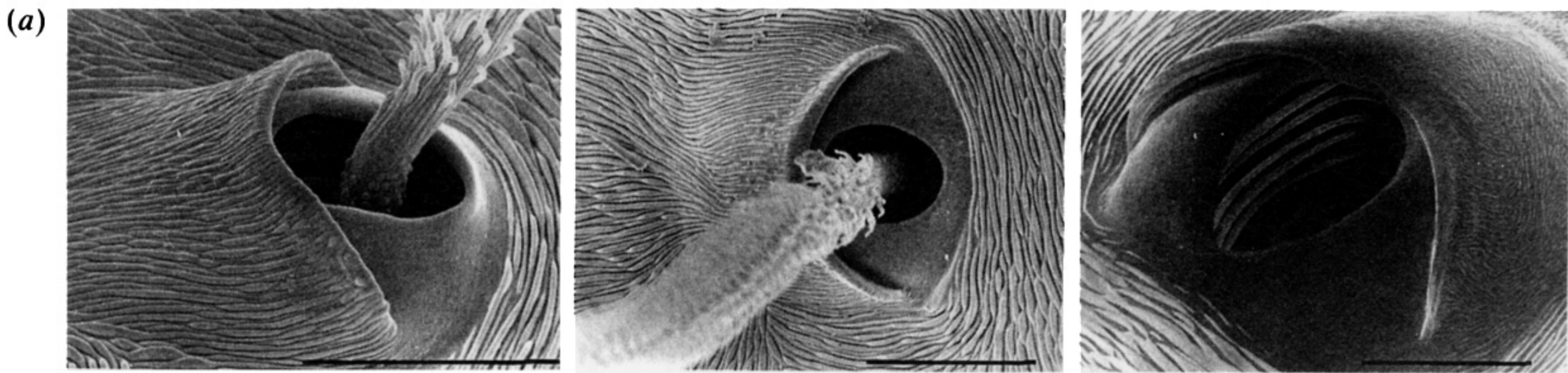
$\alpha = 24° – 30°$

7 μm

10 – 15 μm

α

Figure 3. Structure of trichobothrial cup. (a) SEM views of cup of trichobothria of group TiLP (left, middle) and owing cuticular lamellae inside (right); scale 10 μm. (b) Relation between cup length and hair length. (c) chematic longitudinal section through cup of a short (left) and of a long (right) hair. α, maximal angle of hair shaft splacement.
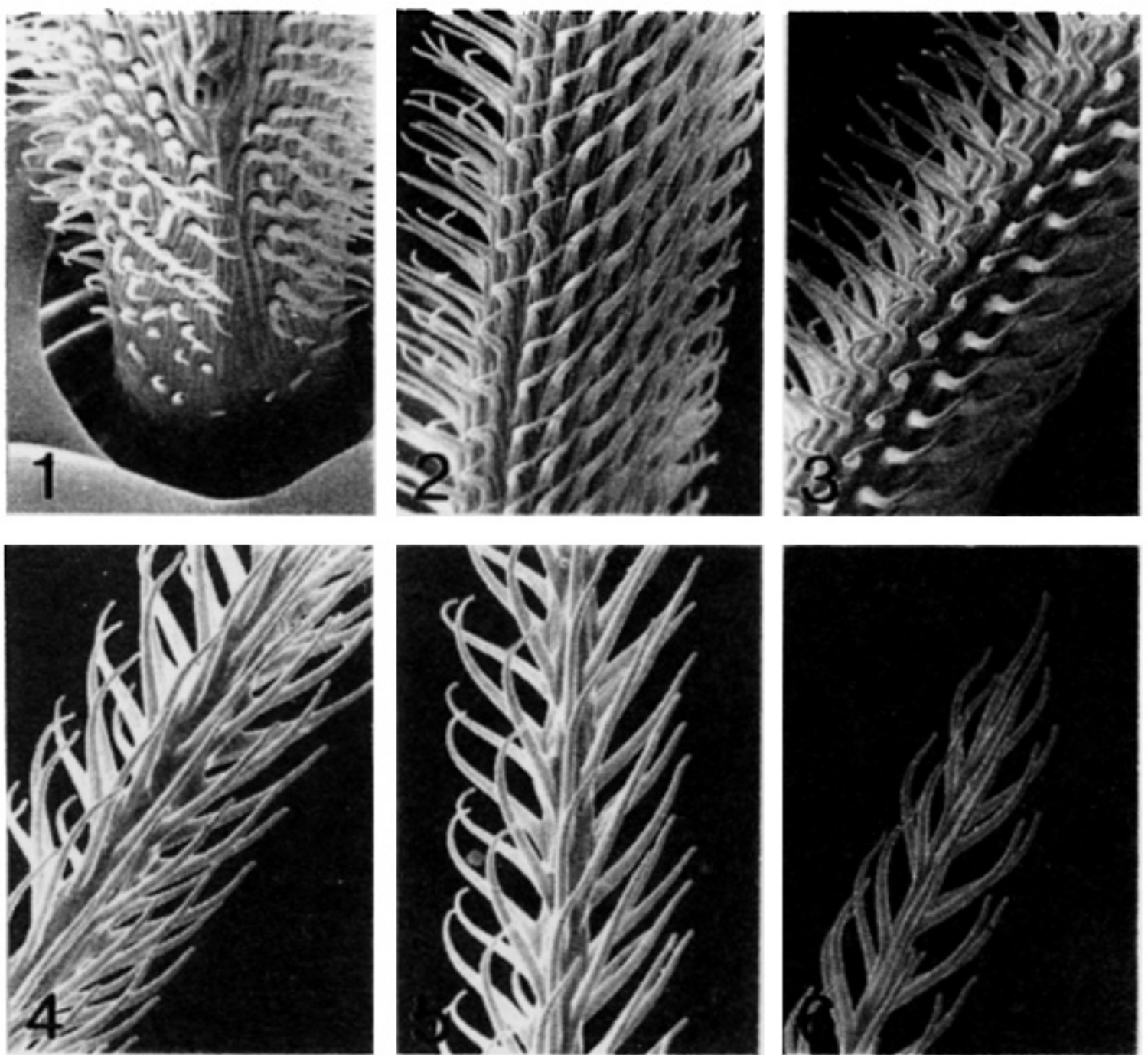
Figure 4. Surface structure of hairshaft. Photographs taken
different levels starting in cup (1) and ending at tip (6) of
ir. Magnification ×1900.